Investigating the Ubiquitous Presence of Nanometric Water Films on Surfaces

Sergio Santos,* Carlo Alberto Amadei, Chia-Yun Lai, Tuza Olukan, Jin-You Lu, Josep Font, Victor Barcons, Albert Verdaguer,* and Matteo Chiesa*

Read Online

ACCESS | Metrics & More | Article Recommendations

ABSTRACT: When we speak of nanometric water films on surfaces we are speaking about a truly ubiquitous phenomenon in nature. All surfaces exposed to ambient conditions are covered by a thin film of water that affects or mediates surface chemistry, general physical-chemical processes on surfaces, and even solid−solid interactions. We have investigated this phenomenon for over a decade by exploiting dynamic atomic force microscopy and have (1) described how these layers affect apparent height measurements, (2) analyzed the excitation of subharmonics, (3) investigated its effects on surface functionality over time ("aging"), (4) monitored and quantified the time-dependent wettability of several relevant surfaces such as highly oriented pyrolytic graphite and monolayer systems, and (5) developed high-resolution and highly stable modes of imaging. Here, we discuss these findings to elucidate the present and future of the field. We further provide a brief but general discussion of solvation and hydration layers in vacuum, liquid, and air that center around current controversies and discuss open possibilities in the field.
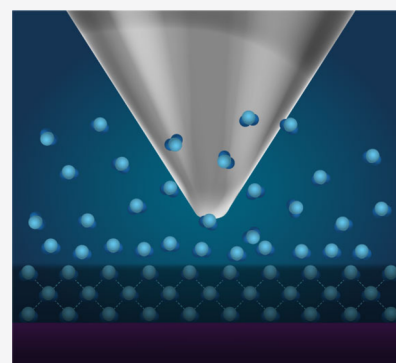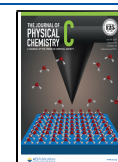
I. INTRODUCTION

The accumulation of molecules such as hydrocarbons and water on surfaces leads to the formation of a thin nanometric interface that mediates and even regulates solid−medium interactions.[1−3] This interface results in the so-called set of interfacial properties,[4,5] that is, electronic, thermal, physico-chemical, and general adhesion, and effectively modifies or indeed establishes the set of surface properties that constitute or give place to the final material structure with the accompanying set of properties.[6,7] Thus, far from being an artificial and uncommon system, this nanometric interface regulates the solid−medium interactions that are common in nature[8] and most of those that are encountered as everyday phenomena.[6,9] We purposefully speak of a solid−medium interface to emphasize that the solid's surface might be exposed to vacuum, air, or liquid environments acting as the medium, but the presence of water molecules in the proximity of the surface will play a key role in the restructuring and reorientation of hydrogen bonds,[3] dangling bonds, and OH (hydroxyl) groups.[7] Still, rather than considering this interface part of the constitutive final structure of a solid and its surface, it is common in surface science to refer to it as "contamination".[10] This terminology emphasizes the fact that (1) the atomic-molecular structure of a pristine solid surface abruptly terminates at the surface and also that (2) surface properties will change as molecules adhere to it. An example of the latter is the capacitance of highly oriented pyrolytic graphite (HOPG); that is, it has been recently reported to

decrease to up to 70% of its initial value in a matter of minutes after an exfoliation.[11] With regard to the former, some have claimed[12] that adherents like water molecules protect the surface from contamination (hydrocarbons), and hence it is not even clear whether all adsorption negatively impacts surface properties. Some have recently claimed that, rather than being a topic on details about a surface, "this issue of [surface contamination] ... under ambient conditions ... [is] ... a topic of much broader relevance".[13] Here we discuss the presence of nanometric layers and water films on surfaces in ambient conditions with a focus on the advances by our team in relation to (1) apparent height measurements in dynamic atomic force microscopy (dAFM), (2) the excitation of subharmonics, (3) the monitoring of the formation and aging of these films, and (4) the possibilities that the presence of these films offer to imaging with atomic force microscopy (AFM). While our discussion is based on the films, or molecular adsorption, encountered in air or ambient conditions, we provide a brief but general discussion of solvation and hydration layers and, more generally, the adsorption of molecules on surfaces as they age in a given

environment, that is, vacuum, liquid, and air, that centers around current controversies and discuss open possibilities in the field.

II. DISCUSSION

II.i. Brief Introduction to the Adsorption of Molecules to Surfaces. Solvation layers and molecular adsorption in general can be studied in vacuum (here molecules can controllably enter the environment), ambient, and liquid environments. When the solvation layer is constituted mostly by water molecules, the layer is typically termed a hydration layer. Such terminology should not be taken for granted; rather, the following question should be constantly kept in mind: Why would molecules bind or attach, weakly or strongly, orderly and forming a well-defined structure or not, to a surface to form and become a nanometric interface acting between a solid's surface and its medium? Arguably, the driving force is the requirement to reduce the free energy resulting from the abrupt termination of a surface.[14−16] Mingyan et al. argued that,[17] given that "the adhesive interaction strength between a surface and a water film can be as high as the cohesive energy density of water (∼0.1456 N/m)", water molecules might more readily adhere to a surface than to bulk water. This phenomenon has been identified as a competition for water molecules to bind to a surface or accept H bonds. Some have reported asymmetries and modifications in the way a water molecule will accept or donate H bonds after interacting with a surface.[18] Others summarize the governing phenomena of the adsorption of water onto surfaces as water−water and water−surface competing to form the H bonds amidst the ubiquitous dispersion interactions.[19] For the sake of clarity and for the purpose of giving a perspective to this phenomenon we cite in full the definition of solvation force given by Pashley and Israelachvili in 1983: "Thus, it was postulated that some surfaces interact strongly with water giving rise to a layer of 'bound' or at least structurally altered water immediately adjacent to them. Because this water is presumed to have a lower free energy than in bulk, when two surfaces approach each other a repulsive force arises corresponding to the work that must be done to transfer water molecules from this layer into the bulk liquid. This force has been called a 'hydration force' or more generally a 'solvation force' and is equivalent to Derjaguin's 'structural component of disjoining pressure'. The idea that surfaces must reduce their free energy has led to discussing and hypothesizing about the ability of water molecules to form hydration layers and working out their structure for almost a century now".[20] Since then, water molecules have been reported to form well-ordered nanostructures, that is, nanometric ice-like films even in ambient conditions,[21] nanometric hydration layers of high mobility,[22] and a rich variety of combinations in between.[19] In this respect, Carrasco et al. claimed that "experiments and calculations [have] reveal[ed] ... a much more interesting variety and richness of structures for water at interfaces".[23] The role of water at interfaces might also relate to lubrication and add to the complexity of the phenomenon of friction and general tribology.[24] If we maintain that wetting is the capacity of a droplet to spread on a surface and that the surface and droplet will repel each other if they cannot weakly bond or attract each other via surface forces, it becomes clear that the structuring or arrangement of water molecules over a surface will be a thermodynamic process resulting in passivation.[3,4] This explains why contact angle measurements

are used to report the wetting of surfaces but also "as a measure of the chemical activity of the surface".[25] Nevertheless, the establishment of a rigid dichotomy differentiating between hydrophobic and hydrophilic surfaces based on this single parameter, that is, contact angle, might result in an oversimplification of the phenomenon.[6,26,27] The problems of thinking in terms of this dichotomy alone are even more pronounced when considering nanometric films.[14] In short, it is intuitive to think that the contact angle of hydrophobic surfaces such as graphite will increase, that is, surfaces will wet less, when exposed to the air environment by adsorbing hydrocarbon contamination. This is because of two presuppositions.[9] First, that graphite, and also graphene, will more readily attract carbon atoms than water molecules. Second, that water adsorption cannot make a surface less hydrophilic. On the one hand, some findings supported both presuppositions above.[10] On the other hand, the structuring and ordering of water molecules is versatile enough to solvate macromolecules,[8,28,29] so this should not be regarded or described as a surprising issue.[30] Atomistic simulations of wetting properties and water films on hydrophilic surfaces showed a dependence between relative humidity (RH) and surface free energy.[31] This work also emphasizes the fact that the formation of thin films of water ubiquitously lower the surface free energy. Furthermore, it has been recently shown that the surface tension of graphene lowers with wetting.[3,26] Since the dipole moment of water together with its H-bonding capabilities depend on the phase and the environment or molecules with which it interacts, one should not trivialize the possibilities of the structure and dynamics of water[32,33] even when confined or trapped within hydrophobic environments.[32] Moreover, if the role of a solvation layer is to passivate a surface it becomes clear that such layers can only increase the contact angle provided liquid water seeks hydrogen bonds and provided we are discussing the wetting of water, that is, hydrophilic and hydrophobic surfaces. For example, Beaglehole and Christensen found footprints of water films even on slightly hydrophobic silicon surfaces and reported that the well-known Lifshitz theory of van der Waals forces does not hold at separations on the order of a few nanometers from the surface to the medium.[34] The translational and orientational order of water molecules on surfaces was already hypothesized in the 1980s.[35] This illustrates the capacity of water molecules to form a wealth of arrangements,[23] coordinate with neighboring structures, and the availability of, for example, ice polymorphs.[6,36] There currently exist many proposed metrics to characterize and probe water structure[6] (ref 6 and refs therein).

The myriad types of possible arrangements, ordered and structured or not, of water molecules on a surface might mean that water can passivate even hydrophobic materials or reduce the "wetting" properties of hydrophobic materials in unexpected ways. Maybe it is such a wealth of possible arrangements and the structure of water, rather than a lack of rigor in reports, that is still puzzling scientists. For example, Kimmel[14] et al. claimed "surprisingly, the water monolayer on each substrate is hydrophobic and gives rise to nonwetting growth for subsequent crystalline layers". Another interesting example is found by considering how the group led by Salmeron reported in 1995 that polygonal shapes, interpreted as nucleation sites of water films, are found in mica surfaces in ambient conditions. The authors reported agreement with the ellipsometry findings of Beaglehole and Christensen. Others

imaged water film formation on surfaces[37] and explored surface diffusion barriers and shapes of water patches on mica and even graphite surfaces by exposing them to water vapor overnight. They further showed that these patches were mobile, since islands tended "to align along the high-symmetry directions of the graphite crystal underneath."[38] Over a decade later Ostendorf et al.[39] focused on these polygonal shapes, that is, hexagonal moiré structures, to report the growth of potassium carbonate crystallites on mica in air "formed as a reaction product of carbonaceous gases with potassium ions". The adsorption of either water molecules or hydrocarbons on surfaces is still explored, as discussed below, in terms of force reconstruction in dAFM. Considering that recent reports[40] have concluded that even a double layer of graphene on a surface can significantly screen the wetting properties of the surface and rearrange[3] the network of hydrogen bonds near the surface, it further becomes clear that a nanometric hydration layer will regulate the wetting properties of a surface in nonintuitive ways. Recently we exploited first principles in quantum simulations[26] to show that "graphene is near van der Waals opaque but partially transparent (near 60%) to polar (ionic) interactions",[41] while the depth of penetration of the force might increase with stronger interactions such as ionic. Albeit, depending on the underlying substrate, adding a graphene layer might change short-range chemistry, including H bonding. With regard to the structuring and composition of the layering, almost a decade ago, advances in dAFM made it possible for Herruzo at al. to visualize an oscillatory decaying force perpendicular to the solid surface with a 0.3 nm periodicity.[42] The group has published extensively in this field since then.[5,43,44] The authors provide references in their work[5] indicating that there are different interpretations for the layering or solvation structure on hydrophobic surfaces, that is, the formation of ice-like water, the adsorption of air-borne molecules, or the layering of condensed gas molecules. Very recently they have indicated that experimental evidence in this topic is either inconclusive or controversial, and, while they operate in liquid, they then concluded that the spacing between oscillations in force on surfaces like graphite is an indication that organic solvents rather than water molecules constitute the layering. This interpretation assumes that water structures are always composed by an interlayering of 0.3 nm, that is, on mica. On graphite the authors report distances in the range of 0.4–0.5 nm. Recently they reported[43] similar oscillation spacings at the solid–liquid interface of mica by exploring a polar solvent, that is, water, and nonpolar liquid, that is, d (n-octane), solvents. Even more recently they have reportedly mapped the interfacial water structure inside a nanoscale water bridge or nanomeniscus.[45] They also performed density functional theory (DFT) simulations to corroborate their experimental findings and showed the presence of similar differences in spacings between water and nonpolar solvents. As early as 1981 Horn, Israelachvili, and Perez reported[46] the presence of oscillations[20,47] in force near the surface via the surface force apparatus, but they interpreted them as short-range positional ordering rather than "long-range orientational order which characterizes the liquid crystal state". In short, the proposed characterizations,[5,38–40] that is, oscillations in force as measured by AFM force measurements, are a good metric to explore structure and layering with high spatial and vertical resolution. In our opinion, the possibility to reconstruct the force robustly in the attractive regime, a development that has significantly advanced over the past

decade, offers this experimental possibility and opens a new field of research. We also revealed the structure of nanometric water films in ambient conditions with up to five oscillations ranging up to 2 nm from the surface.[48]

For more details on water structure and the theory of molecular adsorption on surfaces we refer the interested reader to the extensive work in the literature[2,6,19] that reviews such findings, including the capillary force and others.[23,49] The rest of the document is dedicated to nanometric water films in air and to the findings of the group in the context of the development of the field.

II.ii. Force Profiles in the Presence of Nanometric Films.

We will assume that nanometric films are present in ambient conditions and that these consist of water molecules. A discussion of the evidence that our group has reported over the years is given in another section. In AFM a sharp tip mounted in a microcantilever is made to interact with the surface. The very tip is typically assumed to be effectively spherical.[50,51] This is convenient for several reasons. To a first approximation we can consider that there are two nanometric films in the system,[52] one on the surface of the substrate and another on the surface of the AFM probe (Figure 1). If the
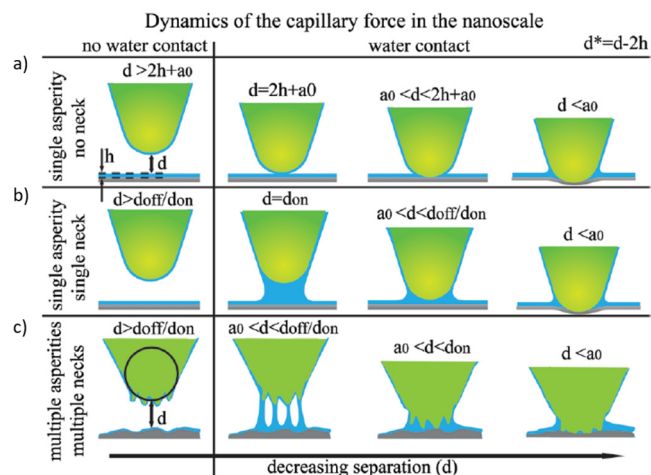

Figure 1. Schemes illustrating (a) a probe identified as a single asperity (top row). Here water layers might be in contact during an oscillation cycle, but the capillary neck does not form. (b) A capillary neck forms and ruptures during one cycle, and (c) the multiple asperities scenario case where several necks might form at sufficiently large separations. The asperities on the tip might lead to repulsive interactions as these make mechanical contact with the sample at different distances d. Reprinted with permission from ref 52. Copyright 2012 American Chemical Society.

distance from surface (tip) to surface (substrate) is termed d and the height of the water layer is termed h, then an effective interaction distance d^* can be defined when $d > 2h$. The main assumption here is that the height of the layer h on the tip coincides with that on the surface (also h). While this is an oversimplification taken for convenience, we might assume that the mean average is h. Then $d^* \equiv d - 2h$ (Figure 1). Several scenarios or force regimes are then possible.

Case One. First one might assume that the tip is a single nanometric asperity with effective radii R (tip radius) and that no water neck or bridge[53,54] forms at any distance from long-range to contact (see top illustration in Figure 1a). In dynamic AFM the cantilever oscillates at or near its resonant frequency ω. In this scenario, for a full cycle, the tip first vibrates

sufficiently far from the substrate, that is, $d > 2h + a_0$, that the interaction is long-range, and the tip and substrate and their water films interact only via long-range van der Waals interactions,[55] where a_0 is an intermolecular distance that implies that there can never be a matter interpenetration.[56] For a discussion of van der Waals interactions the reader can refer to the literature.[56–59] In this long-range regime the forces are typically attractive. It is also typical in AFM to consider $a_0 \approx$ 0.1−0.2 nm as described in surface science textbooks.[4,56] At a distance $a_0 < d \leq 2h + a_0$ the situation is more complex, since the contribution to the attractive component is no longer purely long-range attractive, but rather water films coalesce. Effectively this means that water molecules on both surfaces bond in some way to form a single film.[48,60] An effective value for the Hamaker coefficient $H*$ can be used to model such scenarios.[52] At distances $d \leq a_0$ there is mechanical contact, and the attractive force is identified with the adhesion force F_a. Repulsive contact forces are also present. The illustration of this regime is found in Figure 1 (top).

Case Two. In ambient conditions, a capillary neck might form between the tip, acting as a single asperity, and the substrate (see illustration in the middle row in Figure 1). Some have postulated that a neck forms and ruptures[53,61] during each oscillation in dAFM ($\sim$10−100 k per second). The constant volume approximation might be applicable here, since the condensation from water in the neighborhood of the tip−sample junction might not occur.[54] The main difference here is that, at a distance $d = d_{on} > 2h + a_0$, a neck forms on the tip approach. During tip retraction the neck ruptures at $d = d_{off} > d_{on}$. The result of this hysteretic force is that energy dissipates during each cycle. The abrupt formation and rupture of the neck should manifest in the observables and the force profiles. Methods to compute the theoretical values of d_{on} and d_{off} can be found in the literature.[53] A very thorough review on capillary forces was produced by Butt and Kappl.[49] It might be worth noting that the recent work by Uhlig and Garcia[45] has provided some evidence that the capillary forms and ruptures in the 100 kHz range, that is, in the range that is standard to probe in dynamic AFM. The authors even conclude that there is condensation of liquid from vapor (lower free energy barrier) and also structuring of water from vapor (higher free energy barrier)[62] in these time intervals. It is worth noting however that the formation and rupture of the nanomeniscus in relation to its equilibration in the microsecond time scale is not trivial.

Case Three. We further hypothesize and qualitatively discuss the case of multiple asperity. If the tip is relatively large, that is, $R > 10$−30 nm, it is possible that the probe interacts with the substrate via multiple asperities and that multiple nanometric bridges form. This case is illustrated in the bottom row in Figure 1, but to our knowledge it has never been carefully investigated in AFM. We advance however that a different force profile and differences in observables should follow in these cases. Arguably a **case zero** should be considered, where there are no nanometric films present. This situation is illustrated in Figure 2b (dotted line). A recent review on water adsorption and capillarity in ambient conditions also discusses the problem of multiple neck formation due to multiple asperities.[19] Finally, some have developed models for the multiasperity case in studies of friction, meniscus formation, and wettability showing considerable agreement with experiments.[63]
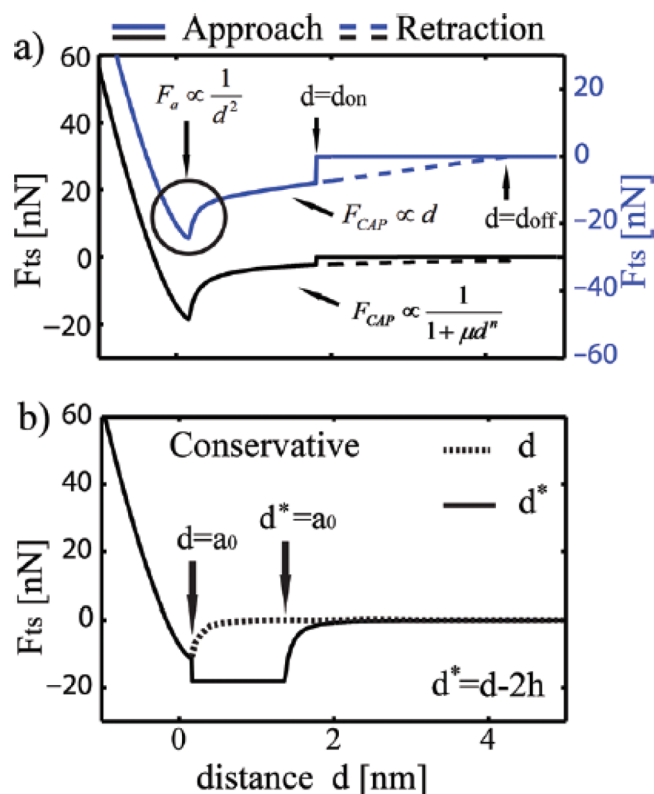

Figure 2. Illustration of the different force−distance F_{ts} dependencies for (a) standard models where F_{ts} displays peaks at close proximities of the surface as predicted by capillary neck formations and rupture and (b) for a conservative system where water might (continuous line) or might not (dotted line) be present. Reprinted with permission from ref 52. Copyright 2012 American Chemical Society.

For a cantilever oscillating at an amplitude A, the stability is related to both the driving force F_D and the average stored energy E_c[64]

$$E_c \approx \frac{1}{2} kA^2 \tag{1}$$

where k is the spring constant. Provided the energy per cycle entering the cantilever via the driving force E_D is much smaller than E_C, that is, $E_D \ll E_c$, something typical in dAFM, the stability is mostly controlled by E_c. If the energy dissipated by the formation and rupture of the water bridge is identified with the work done by this force per cycle, that is, W_{CAP}, a parameter P can be defined that informs of the stability of oscillation.[64]

$$P_c \equiv \frac{W_{CAP}}{E_c} \tag{2}$$

When P_C is small, harmonic motion should follow, but values of P_C close to 1 imply that harmonic motion is compromised due to capillary interactions. The hysteretic nature, that is, $d_{on} \neq d_{off}$, of the capillary force might also induce chaotic regimes.[64,65] Capillary forces due to neck formation are theorized to be proportional to d, but they can also follow more complex relationships.[52] In Figure 2a we illustrate different candidate force profiles, where the net force is written as F_{ts} (tip−sample or substrate). The illustrations of Figure 2a would be identified with Case Two above with the understanding that the capillary force (F_{CAP}) acts in the hysteretic fashion as described. In Figure 2b an illustration is provided of

Case One above. A more detailed discussion of these profiles is out of the scope of this work, and the reader is referred to the literature.[19,52,64]

Almost a decade ago[52] we postulated the existence of a plateau in the force in the proximity of the surface. Experimental amplitude and phase distance curves (APDs) were obtained for a set of samples, that is, quartz and aluminiun. In the simulations the motion of the cantilever was modeled assuming a governing equation of motion consisting of a standard mass on a spring with viscosity in the medium characterized by a Q factor.[52] The forces used in the simulations were constrasted to those predicted by standard models (Figure 2a). It was impossible to reproduce the experimental results by employing forces of the type predicted in Figure 2a, but we could reproduce them when using profiles as in Figure 2b. We further note that the attractive part of the force is convex, as found in our initial experimental work by reconstructing the force,[66] and that this has been consistently corroborated since then.[67−70] The actual shape of the experimental curve[71] was more thoroughly incvestigated and compared to the standard power laws predicted by models in ref 64.

II.iii. Subharmonics and the Dynamics of the Cantilever Inside the Hydration Layer. When the AFM microcantilever is made to vibrate over the surface in air several possibilities arise that can be simplified by considering the drive force alone. In amplitude modulation (AM) AFM the drive force is constant, and the perturbed amplitude A is typically employed to maintain a set-point for feedback and for the extraction of topography; that is, the z-piezo moves vertically to maintain A constant by varying the cantilever distance z_c (Figure 3). Under these conditions the free amplitude A_0 highly influences the regimes of operation in dAFM. For sufficiently small values of A_0, that is, ~1 nm, the tip interacts with the substrate via long-range forces, that is, van der Waals. This is typically termed the attractive regime. For larger values of A_0 the tip starts interacting with the substrate mechanically. When the repulsive forces, that is, unbounded by the phenomenon since the more the tip indents the surface the larger the repulsion, overwhelm the attractive forces, that is, bounded by the phenomenon to a maximum (the force of adhesion), the tip oscillates in the repulsive regime. There is a critical region[53,72] typically termed A_c (critical amplitude) where bistability is present; that is, the nonlinear interaction plus any noise induces switching between a high-amplitude branch of oscillation (or H-state) and a low-amplitude branch of oscillation (or L-state).[73,74] The two states (Figure 3), that is, L and H, coexist for a set of cantilever-operational parameters as shown in the simulation of an amplitude distance (AD) curve in Figure 3a.[75] Nevertheless, in the presence of nanometric films or hydration layers there is another possible regime, namely, the regime of perpetual contact with the water films. We termed this regime of imaging SASS for Small Amplitude Small Set-point.[76] A region of negative slope in amplitude, that is, N, is also shown in the illustration, but this regime is not reachable in standard AM AFM, since this operation mode depends on positive slopes.

In terms of the capillary force, simulations show,[64,65,77] as illustrated in Figure 4a,b, that, in situations where the bridge never forms, that is, d is always larger than d_{on}, the fundamental frequency f, or ω, and the corresponding amplitude A contain most of the energy of the vibrating cantilever. Nevertheless there are situations where the capillary bridge forms and
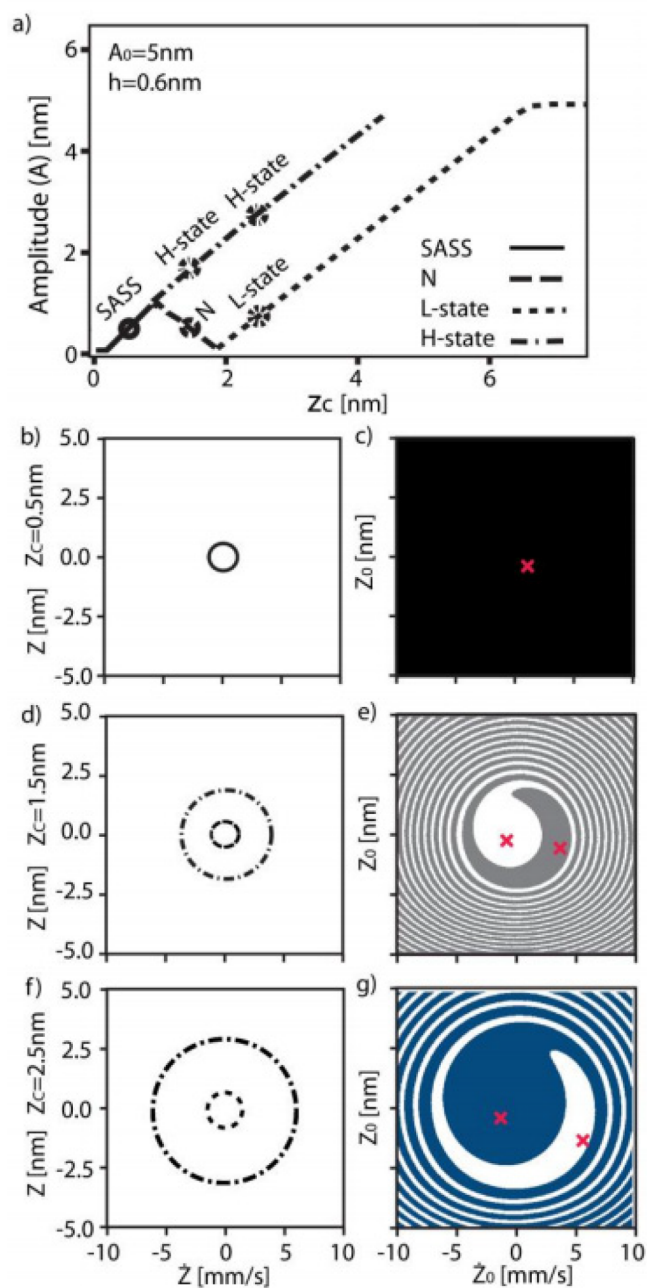

Figure 3. Simulations. (a) Simulated AD curve, where the L and H states and the N and SASS regions are observed. In the left column (b, d, f), the limit cycles $(z,\dot{z})$ for z_c = 0.5, 1.5, and 2.5 nm are shown. The vertical axis is the instantaneous tip position; z and the horizontal axis is the instantaneous tip velocity, $\dot{z}$ in the steady states. Where there are two ellipses, two limit cycles coexist. In the right column (c, e, g), the respective basins of attraction $(z_0, \dot{z}_0, t_0 = 0)$ are shown. These are colored in black (SASS), gray (N region), blue (L state), and white (H state). The Poincaré sections are marked with red crosses. Reprinted with permission from ref 75.

ruptures but not necessarily so during every oscillation cycle (Figure 4c,d). In these situations the fundamental period of oscillation does not coincide any longer with the driving frequency; that is, subharmonics are excited. When there is always contact between the water layers and/or the capillary is always formed, stability returns (not shown in the figure). This is the SASS region as discussed in the context of Figure 3.
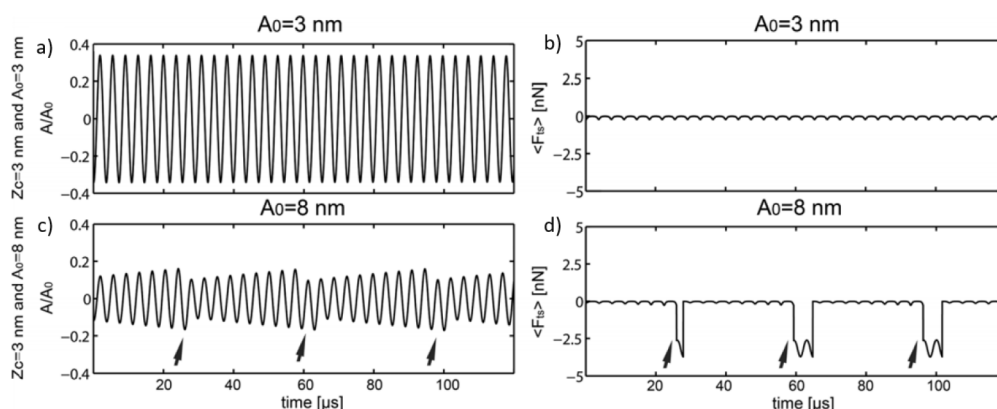
Figure 4. Simulations. Wave forms for (a) the normalized oscillation amplitude $A = A_0$ and (b) the net tip−surface force F_{ts} at $z_c = 3$ nm for $A_0 = 3$ nm. These waveforms correspond to noncontact oscillations. The oscillation amplitude is highly sinusoidal, and the force form presents no peaks. When the free amplitude is increased to $A_0 = 8$ nm (c, d) the oscillation amplitude is modulated by lower frequencies, and the F_{ts} waveform presents peaks corresponding to water impacts. The points at which the tip impacts the water layers are indicated by arrows. Reprinted from ref 64. Copyright 2011 AIP Publishing.
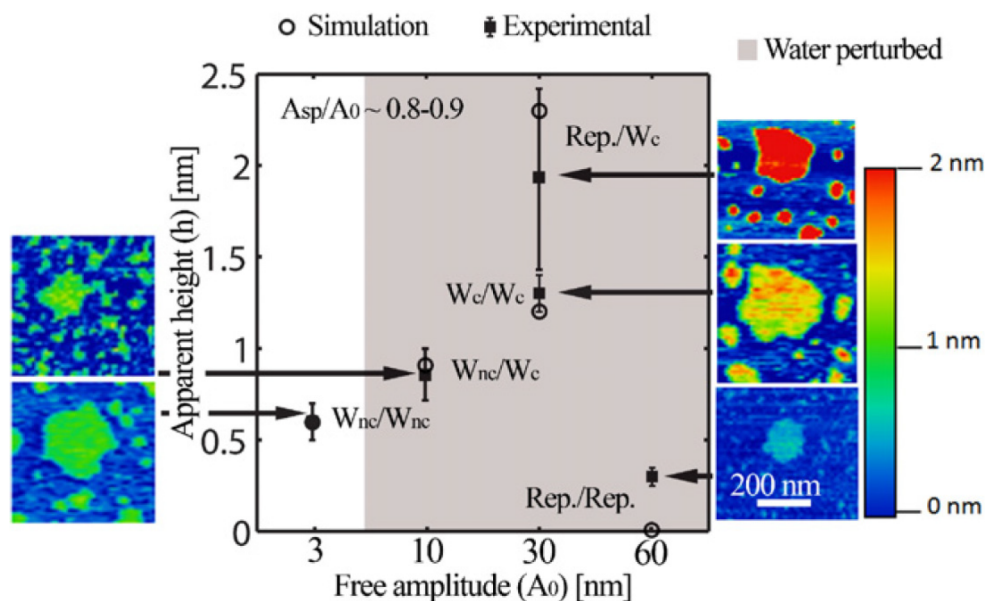

Figure 5. Experimental vs simulation values for the apparent height (h) of water patches on a BaF$_2$(111) sample displaying both wet and unwet regions. The y-axis shows the values of apparent height in nanometers, and in the x-axis the four types of interactions are described. The four types of interactions predicted by the simulations (outlined circles) are experimentally (filled squares) observed to follow similar patterns in terms of the apparent height. Reprinted with permission from ref 55. Copyright 2011 IOP Publishing.

II.iv. Apparent Height and Imaging near or under the Hydration Layer. The different force regimes indicated in the previous section have been experimentally investigated by the group to (1) probe the stability in each imaging regime, (2) monitor the difference in apparent height as measured in dAFM, and (3) probe the possibility to image under the different conditions available. The concept of critical amplitude A_c in relation to the free amplitude A_0 can be employed to provide an experimental basis to probe each regime.[55] Several regimes of interaction were investigated by experimentally probing a BaF$_2$(111) surface. Water molecules show high diffusion on these surfaces, and defects or steps enable the formation of well-defined water patches. This system thus offers the possibility to probe force regimes between the tip and wet and unwet regimes. The regimes are discussed in detail in our work,[55] but a brief summary is provided here in the context of Figure 5. To interpret these figure we adopt the

following terminology; that is, we write interactions as pairs where a first term refers to the tip−hydrophobic pair (dry or unwet regions of the BaF$_2$(111) surface) and a second term to the tip−hydrophilic (or wet) pair. Furthermore, three regimes, other than the SASS regime to be discussed next, can be identified: W_{nc}, W_c, and Rep. We write W_{nc} when there is never water contact, that is, W for water and nc for noncontact (tip or substrate). We write W_c when there is water contact, that is, contact (water on the tip or on the substrate). We write Rep when there is mechanical contact, that is, repulsive. In this case if there is water on the tip or on the substrate there is clear water contact. In the BaF$_2$(111) scenario several possibilities have been identified.

Case 1. The water layers are never perturbed.

Experimentally the W_{nc}/W_{nc} regime for the BaF$_2$(111) scenario can be probed by maintaining the free amplitude
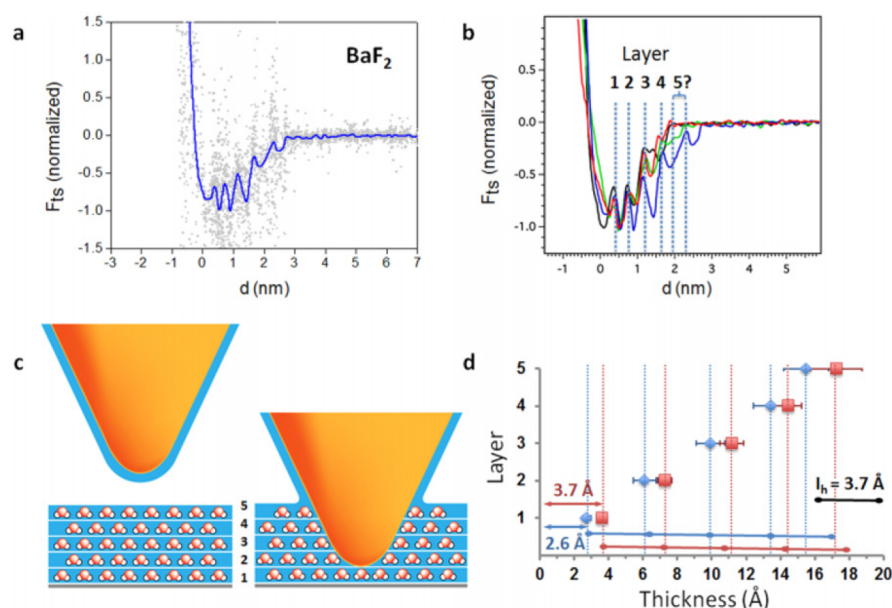
Figure 6. (a) Reconstructed force curve through a water patch on a BaF_2 (111) surface (gray dots, raw data; blue lines, data after smoothing). The curve is normalized with respect to the absolute of the maximum adhesion force $F_{AD} = -2.5$ nN. (b) Series of overlapped force curves on the same water patch. Up to five oscillations are observed with matching positions of the maxima. (c) Scheme showing the AFM tip penetrating five ordered layers of water. (d) Average thickness of the water layers measured as the distance between two consecutive minima in oscillations. Thicknesses are compared with the expected value for an I_h bilayer. Two sets of data are shown depending on the thickness of the first layer, that is, the distance of the first minimum from the onset of mechanical contact ($d = 0$) (2.6 Å in blue or 3.6 Å in red). Reprinted with permission from ref 48. Copyright 2015 American Chemical Society.

sufficiently small; that is, $A_0 \ll 1/2A_c$ (experimental verification in Figure 5).

Case 2. The water layers are perturbed (tip or substrate).

Experimentally several possibilities are available for the $BaF_2(111)$ system, that is, W_c/W_{nc}, W_c/W_c, Rep/W_c (experimental verification in Figure 5). These cases are experimentally accessible when $A_0 \approx 0.5-1A_c$.

Case 3. The water layers are always perturbed if present, since there is mechanical contact with the substrate in each oscillation throughout.

Experimentally we find the case Rep/Rep as shown in Figure 5. This scenario is experimentally accessible when $A_0 \gg A_c$.

Figure 5 shows predictions of the apparent height h of water layers in the simulations as a function of imaging regime. The actual height h was 1 nm in the simulations. In the figure, the predictions of the simulations (outlined circles) are compared to the experimental behavior of the apparent height according to each regime of operation (filled squares). All the data where surfaces are said to have been aged are assumed to have been exposed to ambient conditions for the AFM experiments. Ambient conditions here means RH $\approx 40-60\%$, unless otherwise specified, and $T \approx 20-25\ °C$. We did not conduct experiments to clarify the exact role of RH or temperature. In our experience, however, the aging process is not one where RH alone will alter the surface in a matter of minutes or even a few hours. The reader can refer to ref 82 for details on the preparation. As we show throughout, variations in force as acquired via AFM are detected for at least 24 h after exfoliation; that is, mica and graphite are examples. FTIR absorbance spectra show variations in the region associated with water molecule vibrations for similarly treated samples (see the Discussion on the aging of surfaces).

The height contrast inversion was further investigated by an experimental probe of self-assembled monolayers (SAMs) of

stearic acid (hydrophobic) grown on (hydrophilic) freshly cleaved mica surfaces. The assumption was that water did not adhere on the hydrophobic stearic acid SAMs grown on hydrophilic mica surfaces. Experiments were performed at different RH values.[78] A height contrast inversion resulted as predicted by the simulations; that is, the apparent height of the SAMs was negative in some scenarios. We concluded that the presence of nanometric water layers on mica was responsible for the height inversion. It could be argued that the stearic acid patches (SAMs) on mica are much more compliant than mica and that they might deform under the tip sample interaction. Furthermore, SAMs weakly bind to the mica surface. To elucidate whether this possibility was the cause of height inversion we exploited AM AFM force reconstruction.[79] In particular, Katan and Oosterkamp introduced a robust technique in 2008 and demonstrated its use to probe hydrophobic interactions under pure water (Katan and Oosterkamp 2008). Their Figure 5 showed a plateau for the hydrophilic sample, that is, mica, similar to the one we later hypothesized by comparing simulations of APDs to experimental curves in air. They reported that van der Waals forces alone could not account for the peak in adhesion at ~ 1.5 nm from the mechanical surface, but the force in hydrophobic samples also displayed larger-range attractive forces. They presented the method in air in 2009[80] and acknowledged support from Jarvis and Sader,[81] who derived an equivalent technique for frequency modulation (FM) AFM in 2004. We termed this method the Sader–Jarvis–Katan (SJK) formalism and implemented it in 2013 to investigate the aging of surfaces[66] and the formation of hydration layers[82] in ambient conditions among others (discussed next). For the purpose of stearic acid on mica, our data showed different scenarios when acquiring force data, but our results showed that a height inversion was possible without irreversibly deforming the

samples; that is, height reversion was a consequence of the nature of the forces and AFM probing. It is worth mentioning that investigating smooth transitions in force is possible in the SJK formalism in air, that is, the jump to contact can be avoided.[66]

In 2015[48,60] we performed experiments on BaF_2 (111) surfaces displaying wet and unwet regions (see discussion above in relation to Figure 5) and CaF_2. The lattice constant of BaF_2 (111) is close to the distance of the facing water molecules in hexagonal ice I_h, and the force profiles (also normalized) showed oscillations in the attractive regime with a periodicity of ∼3.7 Å (Figure 6a,b). An illustration showing up to five order layers of water is shown in Figure 6c. The measured thickness according to the number of oscillations measured is shown in Figure 6d. The raw data points are shown in gray in Figure 6a. The data were smoothed, as discussed in the literature,[66] and presented in blue. In the forces acquired on the CaF_2 sample no oscillations were observed, but we reported three distinguishable types of force profiles (not shown). It is worth noting that several types of force curves were found.[48] (1) There is one type where the force decay resembles the well-known inverse-square law, that is, van der Waals type of interactions and with a decay range of 0.5−1 nm. (2) In another the force decays almost linearly. This in relatively good agreement with capillary forces as predicted by the constant chemical potential approximation (see above in the context of Figure 2b). (3) The third profile displayed an attractive force, which is almost constant; that is, it forms a plateau, up to 3−4 nm above the surface.

We have exploited these long-range forces to enhance the resolution of the AFM instrument[76] by operating it in the very close proximity of the surface and with very small amplitudes (i.e., $A ≈ 1$ nm), with the SASS method. In Figure 7a, reprinted from Santos et al.,[76,83] the raw amplitude signal A versus cantilever separation z_c and d_{min} versus z_c are shown. The double helix of a double-standed DNA (dsDNA) molecule imaged on a mica surface cannot be resolved in the nc (or NC) mode of operation (Figure 7b), but it gets resolved when operating in the SASS mode (Figure 7c)—the dsDNA helical periodicity is ∼3.3 nm.[84] This image was acquired in 2010, and force reconstruction via AM AFM methods in ambient conditions were not sufficiently developed or easily implemented,[66,80] but the A, z_c, and d_{min} signals could be recovered by applying simple geometry on the raw signals

$$d_{min} \approx z_c - A \qquad (3)$$

where A and z_c have already been defined and are raw signals easily obtained from AD curves. The concept of d_{min} (or d_m) is meaningful here, since it speaks of a minimum distance of approach per cycle, that is, the closest tip−sample distance. Possible mechanical contact does not lead to ambiguity here, since the reference point $d_{min} = 0$ can always be arbitrarily chosen. Several points are worth noting to understand the effect of water layers on the topography of the dsDNA molecule and on the resolution of the acquired image. First, the nominal height of a dsDNA molecule is ∼2 nm.[84] This height is close to the height predicted for the layers of water that might form on mica in ambient conditions. Second, in the amplitude signal A (black in Figure 7a) there is a region of positive slope that coincides with an abrupt change of slope in the d_{min} signal. This region can be identified with the region where the tip gets trapped in the water layers. After that, another region of positive slope in A follows, that is, the SASS
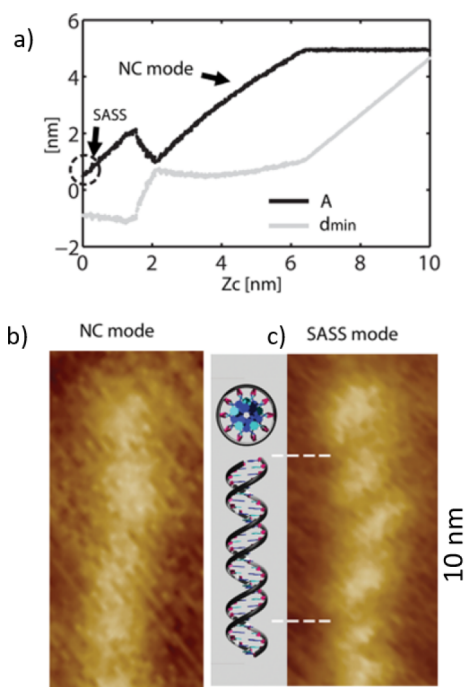

Figure 7. Experimental (a) amplitude A (back lines) and minimum distance of approach d_{min} (gray lines). Experimental examples of images of dsDNA on mica obtained in the (b) NC and (c) SASS modes, respectively. Reprinted with permission from ref 76. Copyright 2013 AIP Publishing.

region. Here d_{min} remains almost constant in that region. The implication is that, in the nc mode the tip oscillates ∼2 nm higher above the surface than in the SASS region for similar values of A. Third, the SASS region is available only for $A ≈ 1−$ 2 nm or less. This is consistent with the fact that, in close proximity with the surface, the tip can only oscillate in permanent contact with the water layer provided the amplitudes are small enough.

The fact that the height of the water layer on mica is predicted to be similar to the nominal height of dsDNA molecules implies that it should be possible to image above the water layers when these form on surfaces as illustrated in Figure 1a. In such cases dsDNA molecules could become "invisible" while imaging; that is, they might not show in topography images. To test this hypothesis we reconstructed[85] force data on freshly cleaved mica, that is, during the first hour after exfoliating the mica, and on the surface of the mica where dsDNA molecules had been deposited for imaging. Since the dsDNA images were taken a few hours after preparation we can term the first case Cleaved mica and the second case Aged mica (aged or treated since the surface is treated by depositing dsDNA molecules with the respective buffer including 2 mM nickel ions). The SASS region was observed in the Aged sample in the amplitude A signal, but it is missing in the Cleaved sample. The A and d_{min} signals only behaved as discussed in the context of Figure 7a in the Aged case. We observed a plateau-like signature in the Aged case only. The hypothesis is that this plateau consists of layers or films of "contamination" or water molecules adsorbed onto the mica surface with time or after depositing the dsDNA molecules. Since the plateau-like feature was measured to be ∼2 nm in length, it follows that it should be possible to vibrate above the surface in the nc mode and above an "invisible" dsDNA

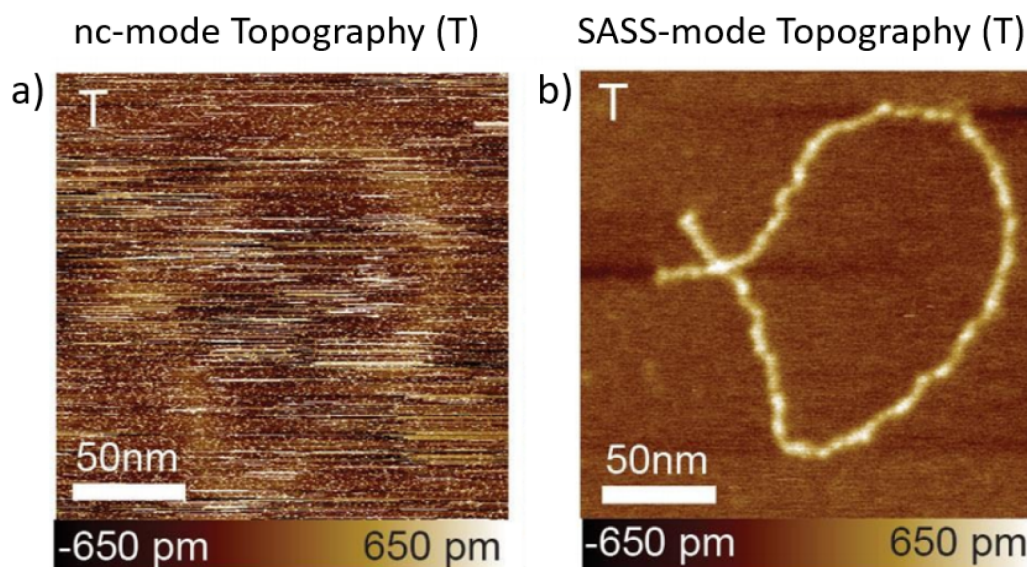## nc-mode Topography (T)   SASS-mode Topography (T)

Figure 8. (a) Topography of a dsDNA molecule (∼1 kbp) for the aged condition. (b) The tip was forced to penetrate the adsorbed thin films by reducing the set point (SASS mode). Reprinted from with permission from ref 85. Copyright 2017 PCCP Owner Societies.

molecule. This situation is experimentally verified in Figure 8a (nc mode), where the topographic image is shown but nothing can be seen. In the SASS mode the tip oscillates ∼2 nm closer to the surface (Figure 8b), and the topography of a dsDNA molecule is resolved. In this case only water layers, rather than the "true" surface, is imaged. According to our interpretation, this provides evidence of (1) the possibility of oscillating in the pure noncontact mode and higher than the water layers and (2) that the water layers are of a similar height as that of the dsDNA molecule, that is, 2 nm. A "plateau" in force of ∼2 nm can be observed in experimentally reconstructed force profiles (Figure 9a) on graphite. Similar plateaus are found for mica surfaces.

II.v. Aging and Force Profiles: The Hydration Layer and Airborne Contaminants. We have thoroughly investigated the evolution of the tip−sample force as it varies in time as samples are exposed to the air environment for several years.[66,67] Much of our work is on graphite,[82] graphene,[41,86] calcite,[27,87,88] and Si substrates.[27] Our results have been interpreted and corroborated by exploiting attenuated total reflectance infrared spectroscopy (ATR IR),[86] Fourier-Transform IR (FTIR),[82,89] static (SCA) and dynamic (DCA), advancing and receding,[82] contact angle measurements, surface free energy,[41] and DFT calculations.[27,90] Some of the results are discussed next with the help of Figures 9 and 10. All of the work assumes that the environment is air.

From the initial discussion of the solvation layer and the possible sources of contamination, it is clear that—as recently recalled by some[5] when working in liquid environments—there is controversy as to whether water molecules or hydrocarbons affect (1) the wettability of graphitic surfaces and (2) their aging processes. In short, the interpretation and data referring to the order, structure, and chemical composition of the layers that passivate surfaces as they age remains controversial in both ambient (i.e., air) and liquid environments. Relatively recently we investigated the evolution of freshly grown HOPG surfaces exposed to a controlled environment,[89] that is, solely containing airborne water or water vapor, as a possible source of contamination (Figure 9).
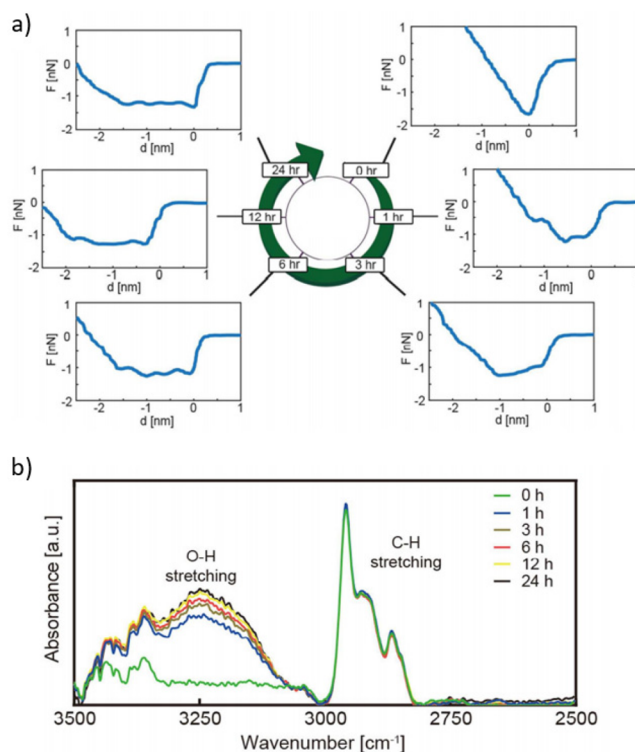

Figure 9. (a) Graphic representation of the evolution of adsorbed water on a graphitic surface as a function of time and (b) FTIR absorbance spectra for a freshly cleaved graphite sample (green line), 1 h (blue line), 3 h (brown line), 6 h (red line), 12 h (yellow line) and 24 h (black line) under controlled temperature and RH in a N_2 environment at 1220 Pa for 24 h (temperature at 23 ± 2 °C and RH ≈ 55 ± 5%). (insets) Absorption peaks of hydrocarbon (C−H stretching) and water (ice-like and liquid-like). The main differences between the spectra lie in the region associated with water molecule vibrations (3100−3600 cm^{-1}), while no apparent differences are recorded for the major peaks belonging to the C−H stretching between 2850 and 2950 cm^{-1}. Reprinted with permission from ref 89. Copyright 2018 PCCP Owner Societies.
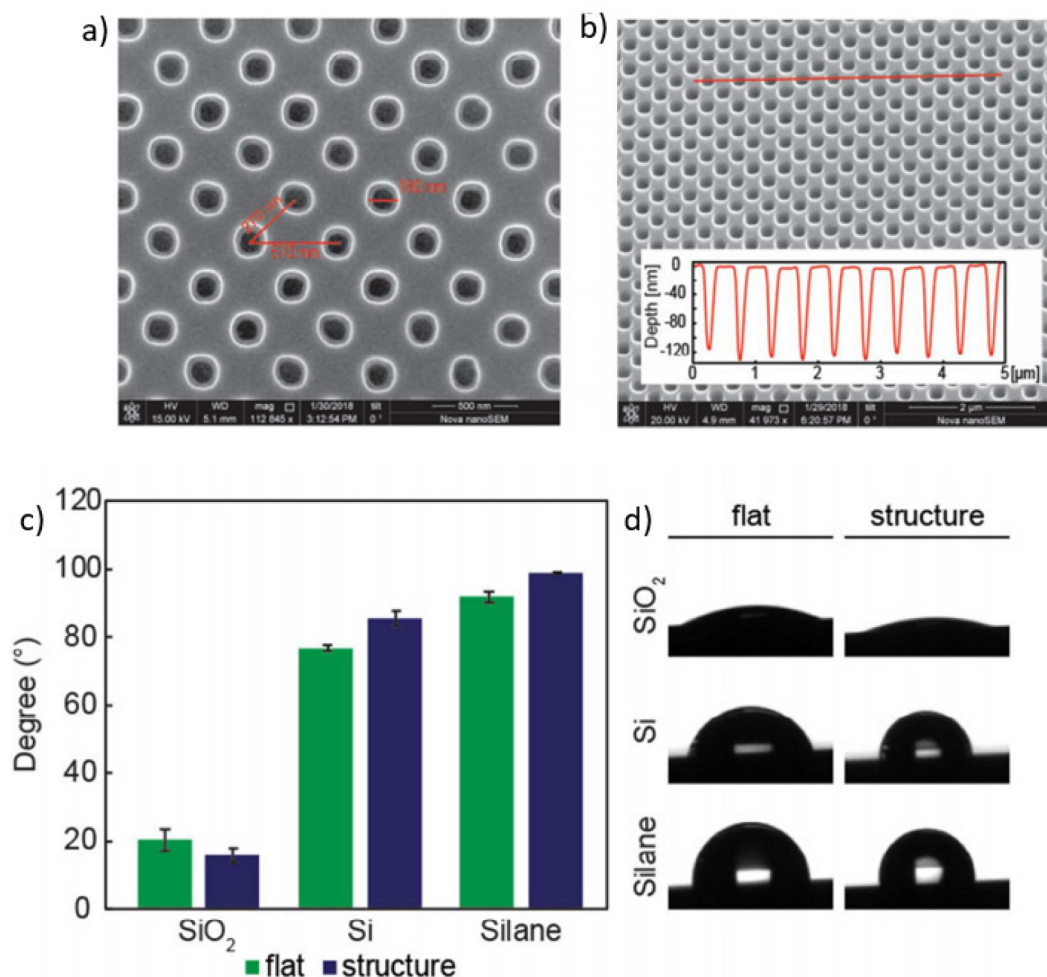
Figure 10. (a) Lattice of pores on a Si substrate acquired by SEM. (b) Topographic AFM scans of the functionalized surfaces. (c) Average values for static contact angles of a 1 μL deionized (DI) water droplet. (b) Photograph of the spreading of the 1 μL of DI water placed on flat and periodically staggered (structure) SiO_2, Si, and silane-functionalized substrates. Reprinted with permission from ref 27. Copyright 2018 American Chemical Society.

The experiments were designed to (1) shed light on the role that airborne hydrocarbons and water adsorption have on surface properties and to (2) provide information regarding the chemical composition of the layers formed when passivating the surfaces. The evolution of the force profiles under a controlled environment are reproduced in Figure 9a for the 0th to the 24th hour after cleavage. The profiles are qualitatively shown to transform. We already reported that several types of force profiles are possible in samples like CaF_2 crystals.[48] The interpretation given in ref 43 is thus also meaningful for the interpretation of Figure 9. Further details can be found in the literature.[48,89] The chemical composition of the surface and its possible modification has been analyzed by means of FTIR (Figure 9b). According to our data,[41] the adhesion force F_{AD} approximately halves within the first hour of exposure;[26] then it is maintained throughout (Figure 9a), and only the shape of the curve changes. This experimental finding was corroborated in the DFT simulations.[26,41] In the FTIR figure, the green line represents the FTIR molecular fingerprint of a freshly cleaved HOPG surface, and the black line refers to a sample exposed to humidity for 24 h. Our interpretation of the data is that, if hydrocarbon adsorption on graphite is to correctly explain the aging process and the variations in wettability of graphite, this must occur

immediately after cleaving, that is, less than 5 min after cleavage, since this is the time between the HOPG exfoliation in ambient and the acquisition of the first spectra in the controlled organic free environment of our diffuse reflectance infrared Fourier transform (DRIFT) FTIR system.[89] The C–H peaks occur between 2850 and 2950 cm^{-1} in the spectra, and they are possibly attributable to hydrocarbon contamination. Variations more readily occur in the 3100–3600 cm^{-1} range, where O–H stretching vibration takes place after the first 5 min of exfoliation.

We have further extensively exploited DFT computation[26,41] to show that it is possible for layers of water molecules to adhere to graphitic surfaces while increasing the contact angle, that is, reducing the surface free energy (not shown but discussed in detail in refs 26 and 37). This agrees with the hypothesis that surfaces must reduce their surface free energy in order to thermodynamically passivate,[82] that is, reduce, their reactivity with time. To corroborate our DFT results graphitic surfaces were exposed to ambient conditions and to controlled environments where only water molecules, that is, water vapor, were present in the enclosed environment as discussed in the context of Figure 9. The static contact angles were measured for the same conditions.[26] The initial contact angle was recovered by an annealing of the surface. These results agree

with our initial findings in 2014.[82] While it is not intuitive to think that water absorption can make a surface more hydrophobic, we recall that it is liquid water competing with the surface-bound water that is at stake. These are two competing mechanisms as previously discussed,[3] and such findings and interpretations agree with the DFT calculations.

To conclude, we briefly mention that most of the work we have reported so far relates to the wetting behavior of homogeneous systems at the macroscopic scale. In order to understand the role of morphology over against chemical composition and structure on wetting properties a simple system was manufactured. A two-dimensional square lattice of pores on Si, silane, and SiO_2 substrates was manufactured for the experiment. The characteristic diameter is ∼180 nm, and the lattice constant values are 510 and 270 nm, respectively, as shown in Figure 10a. Topographic AFM scans were taken to show depths in the order of 100 nm (Figure 10b). These are enough to decouple chemistry from the morphology in the nanoscale. The manufactured structured can be produced in a way that the ratio between the flat region and the pore on the plane of the surface, that is, Si, silane, or SiO_2, can be varied as shown in Figure 10c. The contact angle results are showcased for each case in Figure 10d. As expected, the contact angle increased with porosity, that is, lack of flatness, indicating that wettability as quantified by contact angle measurements is highly dependent on the porosity. We also showed (not shown) via force distance measurements that nanoscale properties such as adhesion were indeed not modified by adding/removing structure to the surfaces. The possibility to monitor the nanoscale behavior, that is, the very surface of the samples with high spatial and vertical resolution, allowed us to investigate the role of morphology alone fully decoupling it from chemical modifications of the surface.

III. CONCLUSION

In summary, we have presented the field of the adsorption of molecules on surfaces in air by providing a general overview of current theories and findings with a focus on AFM experiments. While several recent breakthroughs have allowed us to visualize the chemical composition and structure of water with high spatial and vertical resolution with the AFM, there is still controversy in the field in terms of order, structure, and chemical composition and in relation to the solvation and/or hydration layers in vacuum, liquid, and air. It is not clear to us whether the differentiation of surfaces in terms of the hydrophobic/hydrophilic dichotomy alone is sufficient to elucidate the properties and behavior of surfaces exposed to air environments in relation to the structuring and layering of water molecules on surfaces. Throughout this work the question as to why molecules would bind or attach to a surface to form and become a nanometric interface acting between a solid surface and its medium has led the discussion. In the positive, we have discussed molecular adhesion in air environments and have provided evidence via dAFM measurements, contact angle measurements, DFT calculations, and FTIR spectroscopy regarding (1) the fact that the tip−sample force undergoes important qualitative and quantitative changes for all surfaces under investigation for several hours after the creation of the surface—from HOPG and graphene (hydrophobic) to $BaF_2(111)$, mica, and calcite (hydrophilic), (2) the different values in the apparent height of nanostructures, that is, nanometric films such as stearic acids (SAMs), nanometric water patches such as those formed on $BaF_2(111)$ and calcite,

and macromolecules such as dsDNA that can be measured in dAFM depending on operational parameters and the presence of adsorbed molecules on a surface, (3) the different force regimes that become available when imaging in air, including the possibility to excite subharmonics, (4) the oversimplification that results from thinking of water bridges spontaneously forming between the tip and the surface only rather than also considering the possibility of adsorption of molecules onto surfaces with time, and (5) the possibility of imaging with very small amplitudes, that is, $A_0 \approx 0.1−1$ nm, in the very proximity of the surface in ambient conditions by exploiting an "anomaly" in the standard behavior of the amplitude A signal in dAFM in air. In terms of our discussion of imaging in air by exploiting this anomaly, others have also shown similar possibilities while imaging with a cantilever based on a quartz tuning fork (qPlus sensor)[91] in FM AFM. Still, while they emphasized the ubiquitous presence of water films on surfaces in ambient conditions by referring to a well-established textbook in surface science,[4] an emphasis was put on relative humidity alone rather than on surface aging and the role of passivation with time. It is unclear to us whether the authors exploited the same anomaly, but the example shows that the field of the adsorption of water molecules on surfaces in air still offers many possibilities for research. In particular, such interpretations show that there is a tendency to think of water adsorption on surfaces in air by considering relative humidity alone. In this sense, our main contribution is the consideration that water might strongly bind to surfaces with time and become part of the solid.

■ AUTHOR INFORMATION

Corresponding Authors

Sergio Santos − *Department of Physics and Technology, UiT-the Arctic University of Norway, Tromsø 9037, Norway;* orcid.org/0000-0003-0448-1668; Email: ssantos78h@gmail.com

Matteo Chiesa − *Department of Physics and Technology, UiT-the Arctic University of Norway, Tromsø 9037, Norway; Laboratory for Energy and NanoScience, Khalifa University of Science and Technology, Abu Dhabi 127788, United Arab Emirates;* Email: matteo.chiesa@uit.no

Albert Verdaguer − *Institut de Ciència de Materials de Barcelona Campus de la UAB, Bellaterra 08193, Spain;* orcid.org/0000-0002-4855-821X; Email: averdaguer@icmab.es

Authors

Carlo Alberto Amadei − *The World Bank, Washington 20433, DC, United States;* orcid.org/0000-0003-4107-6661

Chia-Yun Lai − *Department of Physics and Technology, UiT-the Arctic University of Norway, Tromsø 9037, Norway;* orcid.org/0000-0002-1758-1118

Tuza Olukan − *Department of Physics and Technology, UiT-the Arctic University of Norway, Tromsø 9037, Norway*

Jin-You Lu − *Advanced Materials Group, Technology Innovation Institute, Abu Dhabi, United Arab Emirates*

Josep Font − *Departament d'Enginyeria Minera, Industrial i TIC, UPC BarcelonaTech, Manresa 08242, Spain*

Victor Barcons − *Departament d'Enginyeria Minera, Industrial i TIC, UPC BarcelonaTech, Manresa 08242, Spain*

Complete contact information is available at:

https://pubs.acs.org/10.1021/acs.jpcc.1c03767

Notes

The authors declare no competing financial interest.

Biographies

Sergio Santos is a Postdoctoral Research Fellow at UiT, Norway, and has over a decade of experience in nanoscale science and technology. He is a specialist in dynamic AFM methods in air. He got his PhD from Leeds University in 2011 on the topic of AFM imaging of macromolecules on surfaces in air.

Carlo Alberto Amadei is a young professional working in the in the Latin America and Caribbean water practice. He is currently supporting water supply and sanitation programs in Ecuador and Dominican Republic, as well as initiatives surrounding water and circular economy. He graduated cum laude in Environmental and Sustainable Engineering from University of Modena and Reggio Emilia (2012) and holds a PhD in Engineering Sciences from Harvard University (2019) where he focused on the use of new emerging materials for wastewater reclamation.

Chia-Yun Lai is currently working with Asylum Research—An Oxford Instruments Company—and got her PhD "Quantitatively reinterpreting atomic force microscopy via the data science paradigm" in 2019 under UiT, the Arctic University of Norway.

Tuza Olukan is a Postdoctoral Research Fellow at UiT, Norway. He holds a doctorate degree in Material Science and Nanotechnology Engineering under the MIT/MI Collaborative Program at the Khalifa University. His scientific interests rest on the deployment of cutting-edge solutions in addressing scientific and technological challenges with an emphasis on low-cost, sustainable, and, locally sourced materials and resources. His current research effort is geared towards adopting multidisciplinary strategies in the decarbonization, decentralization, and digitalization of the electricity sector especially in remote regions of the world and the Global South countries in general.

Jin-You Lu works at the Advanced Materials Group, Technology Innovation Institute, in Abu Dhabi. His research interests include nanophotonics, solar energy conversion application, advanced materials including 2D material properties and their applications, numerical optical simulations, and quantum physics simulation. He got his PhD at the Nanyang Technological University, Singapore.

Josep Font is a Professor at the Polytechnic University of Catalonia (UPC) and acts as a technical advisor to Mur & Martí. He got his PhD in 1992 at UPC, Barcelona.

Victor Barcons is a researcher and lecturer at the Universitat Politècnica de Catalunya (UPC) and got his PhD at UPC in 2014 "Contribution to the characterization of the atomic force microscope". He is an expert in the field of numerical simulations, signal processing, and data interpretation.

Albert Verdaguer is currently working at the Institut de Ciència de Materials de Barcelona (ICMAB) studying water–solid interfaces and ice nucleation. He was graduated in Physics at the University of Barcelona (UB) and obtained his PhD in Physics at the same university studying molecular collective motions in liquids using molecular dynamics simulations. Later, as a postdoc at the Lawrence Berkeley National laboratory, he changed the focus of his research to the study of wetting at the nanoscale using AFM and Ambient-Pressure X-ray Photoelectron Spectroscopy. So far he has been studying water interactions with minerals, metals, self-assembled monolayers, perovskites, or graphene among others.

Matteo Chiesa is the head of the LENS (Laboratory for Energy and Nano Science) at the Khalifa University of Science and Technology in Abu Dhabi and UiT, Norway, and got his PhD from the Norwegian University of Science and Technology (NTNU) in 2001. He is a materials scientist and specializes in the understanding of the atomic and nanoscale interactions that govern the macroscopic functionality of materials. He has recently redirected his expertise in Atomic Force Microscopy (AFM) towards the quantitative investigation of soft materials in living organisms.

REFERENCES

(1) Verdaguer, A.; Sacha, G. M.; Bluhm, H.; Salmeron, M. Molecular Structure of Water at Interfaces: Wetting at the Nanometer Scale. *Chem. Rev.* **2006**, *106*, 1478−1510.

(2) Henderson, M. A. The Interaction of Water with Solid Surfaces: Fundamental Aspects Revisited. *Surf. Sci. Rep.* **2002**, *46*, 1−308.

(3) Chiricotto, M.; Martelli, F.; Giunta, G.; Carbone, P. Role of Long-Range Electrostatic Interactions and Local Topology of the Hydrogen Bond Network in the Wettability of Fully and Partially Wetted Single and Multilayer Graphene. *J. Phys. Chem. C* **2021**, *125*, 6367−6377.

(4) Israelachvili, J. N. *Intermolecular and Surface Forces*; Elsevier Academic Press: London, UK, 2005.

(5) Uhlig, M. R.; Benaglia, S.; Thakkar, R.; Comer, J.; Garcia, R. Atomically Resolved Interfacial Water Structures on Crystalline Hydrophilic and Hydrophobic Surfaces. *Nanoscale* **2021**, *13*, 5275−5283.

(6) Monroe, J.; Barry, M.; DeStefano, A.; Aydogan Gokturk, P.; Jiao, S.; Robinson-Brown, D.; Webber, T.; Crumlin, E. J.; Han, S.; Shell, M. S. Water Structure and Properties at Hydrophilic and Hydrophobic Surfaces. *Annu. Rev. Chem. Biomol. Eng.* **2020**, *11*, 523−557.

(7) Zhou, G.; Li, L.; Peng, K.; Wang, X.; Yang, Z. Wettability Transition on Graphyne-Coated Au(111) Substrates with Different Pore Sizes: The Role of Interfacial Hydrogen Bonds. *J. Phys. Chem. C* **2021**, *125*, 7971−7979.

(8) Tamoliunas, K.; Galamba, N. Protein Denaturation, Zero Entropy Temperature, and the Structure of Water around Hydrophobic and Amphiphilic Solutes. *J. Phys. Chem. B* **2020**, *124*, 10994−11006.

(9) Dreier, L. B.; Liu, Z.; Narita, A.; van Zadel, M. J.; Müllen, K.; Tielrooij, K. J.; Backus, E. H. G.; Bonn, M. Surface-Specific Spectroscopy of Water at a Potentiostatically Controlled Supported Graphene Monolayer. *J. Phys. Chem. C* **2019**, *123*, 24031−24038.

(10) Li, Z.; Wang, Y.; Kozbial, A.; Shenoy, G.; Zhou, F.; McGinley, R.; Ireland, P.; Morganstein, B.; Kunkel, A.; Surwade, S. P.; et al. Effect of Airborne Contaminants on the Wettability of Supported Graphene and Graphite. *Nat. Mater.* **2013**, *12*, 925−931.

(11) Hurst, J. M.; Li, L.; Liu, H. Adventitious Hydrocarbons and the Graphite-Water Interface. *Carbon* **2018**, *134*, 464−469.

(12) Li, Z.; Kozbial, A.; Nioradze, N.; Parobek, D.; Shenoy, G. J.; Salim, M.; Amemiya, S.; Li, L.; Liu, H. Water Protects Graphitic Surface from Airborne Hydrocarbon Contamination. *ACS Nano* **2016**, *10*, 349−59.

(13) Lacasa, J. S.; Almonte, L.; Colchero, J. In Situ Characterization of Nanoscale Contaminations Adsorbed in Air Using Atomic Force Microscopy. *Beilstein J. Nanotechnol.* **2018**, *9*, 2925−2935.

(14) Kimmel, G. A.; Petrik, N. G.; Dohnálek, Z.; Kay, B. D. Crystalline Ice Growth on Pt(111) and Pd(111): Nonwetting Growth on a Hydrophobic Water Monolayer. *J. Chem. Phys.* **2007**, *126*, 114702.

(15) Serva, A.; Salanne, M.; Havenith, M.; Pezzotti, S. Size Dependence of Hydrophobic Hydration at Electrified Gold/Water Interfaces. *Proc. Natl. Acad. Sci. U. S. A.* **2021**, *118*, e2023867118.

(16) Li, J.; Wang, J.; Wang, Y.; Lu, D.; Wu, J. A Multiscale Procedure for Predicting the Hydration Free Energies of Polycyclic Aromatic Hydrocarbons. *J. Chem. Eng. Data* **2020**, *65*, 2206−2211.

(17) He, M.; Szuchmacher Blum, A.; Aston, D. E.; Buenviaje, C.; Overney, R. M.; Luginbühl, R. Critical Phenomena of Water Bridges in Nanoasperity Contacts. *J. Chem. Phys.* **2001**, *114*, 1355−1360.

(18) Michaelides, A.; Morgenstern, K. Ice Nanoclusters at Hydrophobic Metal surfaces. *Nat. Mater.* **2007**, *6*, 597−601.

(19) Xiao, C.; Shi, P.; Yan, W.; Chen, L.; Qian, L.; Kim, S. H. Thickness and Structure of Adsorbed Water Layer and Effects on Adhesion and Friction at Nanoasperity Contact. *Colloids and Interfaces* **2019**, *3*, 55.

(20) Pashley, R. M.; Israelachvili, J. N. Molecular Layering of Water in Thin Films between Mica Surfaces and Its Relation to Hydration Forces. *J. Colloid Interface Sci.* **1984**, *101*, 511−523.

(21) Asay, D. B.; Kim, S. H. Evolution of the Adsorbed Water Layer Structure on Silicon Oxide at Room Temperature. *J. Phys. Chem. B* **2005**, *109*, 16760−16763.

(22) Nagy, G. Water Structure at the Graphite(0001) Surface by Stm Measurements. *J. Electroanal. Chem.* **1996**, *409*, 19−23.

(23) Carrasco, J.; Hodgson, A.; Michaelides, A. A Molecular Perspective of Water at Metal Interfaces. *Nat. Mater.* **2012**, *11*, 667−674.

(24) Urbakh, M.; Klafter, J.; Gourdon, D.; Israelachvili, J. The Nonlinear Nature of Friction. *Nature* **2004**, *430*, 525−528.

(25) Hu, J.; Xiao, X. D.; Ogletree, D. F.; Salmeron, M. Imaging the Condensation and Evaporation of Molecularly Thin Films of Water with Nanometer Resolution. *Science* **1995**, *268*, 267.

(26) Lu, J.-Y.; Lai, C.-Y.; Almansoori, I.; Chiesa, M. The Evolution in Graphitic Surface Wettability with First-Principles Quantum Simulations: The Counterintuitive Role of Water. *Phys. Chem. Chem. Phys.* **2018**, *20*, 22636−22644.

(27) Sloyan, K.; Lai, C.-Y.; Lu, J.-Y.; Alfakes, B.; Al Hassan, S.; Almansouri, I.; Dahlem, M. S.; Chiesa, M. Discerning the Contribution of Morphology and Chemistry in Wettability Studies. *J. Phys. Chem. A* **2018**, *122*, 7768−7773.

(28) Clementi, E.; Corongiu, G. Simulations of the Solvent Structure for Macromolecules: Solvation Model for B-DNA and Na+-B-DNA Double Helix at 300 Degrees K. *Ann. N. Y. Acad. Sci.* **1981**, *367*, 83−107.

(29) Grayce, C. J.; Schweizer, K. S. Solvation Potentials for Macromolecules. *J. Chem. Phys.* **1994**, *100*, 6846−6856.

(30) de Gennes, P. G. Wetting: Statics and Dynamics. *Rev. Mod. Phys.* **1985**, *57*, 827−863.

(31) Kanduč, M.; Netz, R. R. Atomistic Simulations of Wetting Properties and Water Films on Hydrophilic Surfaces. *J. Chem. Phys.* **2017**, *146*, 164705.

(32) Tummala, N. R.; Striolo, A. Hydrogen-Bond Dynamics for Water Confined in Carbon Tetrachloride−Acetone Mixtures. *J. Phys. Chem. B* **2008**, *112*, 10675−10683.

(33) Yaron, D.; Peterson, K. I.; Zolandz, D.; Klemperer, W.; Lovas, F. J.; Suenram, R. D. Water Hydrogen Bonding: The Structure of the Water−Carbon Monoxide Complex. *J. Chem. Phys.* **1990**, *92*, 7095−7109.

(34) Beaglehole, D.; Christenson, H. K. Vapor Adsorption on Mica and Silicon: Entropy Effects, Layering, and Surface Forces. *J. Phys. Chem.* **1992**, *96*, 3395−3403.

(35) Du, Q.; Freysz, E.; Shen, Y. R. Vibrational Spectra of Water Molecules at Quartz/Water Interfaces. *Phys. Rev. Lett.* **1994**, *72*, 238−241.

(36) Matsui, T.; Hirata, M.; Yagasaki, T.; Matsumoto, M.; Tanaka, H. Communication: Hypothetical Ultralow-Density Ice Polymorphs. *J. Chem. Phys.* **2017**, *147*, 091101.

(37) Luna, M.; Colchero, J.; Gil, A.; Gómez-Herrero, J.; Baró, A. M. Application of Non-Contact Scanning Force Microscopy to the Study of Water Adsorption on Graphite, Gold and Mica. *Appl. Surf. Sci.* **2000**, *157*, 393−397.

(38) Gil, A.; Colchero, J.; Luna, M.; Gómez-Herrero, J.; Baró, A. M. Adsorption of Water on Solid Surfaces Studied by Scanning Force Microscopy. *Langmuir* **2000**, *16*, 5086−5092.

(39) Ostendorf, F.; Schmitz, C.; Hirth, S.; Kühnle, A.; Kolodziej, J. J.; Reichling, M. Evidence for Potassium Carbonate Crystallites on Air-Cleaved Mica Surfaces. *Langmuir* **2009**, *25*, 10764−10767.

(40) Kim, D.; Pugno, N. M.; Buehler, M. J.; Ryu, S. Solving the Controversy on the Wetting Transparency of Graphene. *Sci. Rep.* **2015**, *5*, 15526.

(41) Lu, J.-Y.; Olukan, T.; Tamalampudi, S. R.; Al-Hagri, A.; Lai, C.-Y.; Ali Al Mahri, M.; Apostoleris, H.; Almansouri, I.; Chiesa, M. Insights into Graphene Wettability Transparency by Locally Probing Its Surface Free Energy. *Nanoscale* **2019**, *11*, 7944−7951.

(42) Herruzo, E. T.; Asakawa, H.; Fukuma, T.; Garcia, R. Three-Dimensional Quantitative Force Maps in Liquid with 10 Piconewton, Angstrom and Sub-Minute Resolutions. *Nanoscale* **2013**, *5*, 2678−2685.

(43) Hernández-Muñoz, J.; Uhlig, M. R.; Benaglia, S.; Chacón, E.; Tarazona, P.; Garcia, R. Subnanometer Interfacial Forces in Three-Dimensional Atomic Force Microscopy: Water and Octane near a Mica Surface. *J. Phys. Chem. C* **2020**, *124*, 26296−26303.

(44) Fukuma, T.; Garcia, R. Atomic- and Molecular-Resolution Mapping of Solid−Liquid Interfaces by 3d Atomic Force Microscopy. *ACS Nano* **2018**, *12*, 11785−11797.

(45) Uhlig, M. R.; Garcia, R. In Situ Atomic-Scale Imaging of Interfacial Water under 3d Nanoscale Confinement. *Nano Lett.* **2021**, DOI: 10.1021/acs.nanolett.1c01092.

(46) Horn, R. G.; Israelachvili, J. N.; Perez, E. Forces Due to Structure in a Thin Liquid Crystal Film. *J. Phys. (Paris)* **1981**, *42*, 39−52.

(47) Christenson, H. K.; Horn, R. G. Direct Measurement of the Force between Solid Surfaces in a Polar Liquid. *Chem. Phys. Lett.* **1983**, *98*, 45−48.

(48) Calò, A.; Domingo, N.; Santos, S.; Verdaguer, A. Revealing Water Films Structure from Force Reconstruction in Dynamic Afm. *J. Phys. Chem. C* **2015**, *119*, 8258−8265.

(49) Butt, H. J.; Kappl, M. Normal Capillary Forces. *Adv. Colloid Interface Sci.* **2009**, *146*, 48−60.

(50) Giessibl, F. J. Advances in Atomic Force Microscopy. *Rev. Mod. Phys.* **2003**, *75*, 949.

(51) Calabri, L.; Pugno, N.; Menozzi, C.; Valeri, S. Afm Nanoindentation: Tip Shape and Tip Radius of Curvature Effect on the Hardness Measurement. *J. Phys.: Condens. Matter* **2008**, *20*, 474208.

(52) Barcons, V.; Verdaguer, A.; Font, J.; Chiesa, M.; Santos, S. Nanoscale Capillary Interactions in Dynamic Atomic Force Microscopy. *J. Phys. Chem. C* **2012**, *116*, 7757−7766.

(53) Zitzler, L.; Herminghaus, S.; Mugele, F. Capillary Forces in Tapping Mode Atomic Force Microscopy. *Phys. Rev. B: Condens. Matter Mater. Phys.* **2002**, *66*, 155436.

(54) Yaminsky, V. V. The Hydrophobic Force: The Constant Volume Capillary Approximation. *Colloids Surf., A* **1999**, *159*, 181−195.

(55) Santos, S.; Verdaguer, A.; Souier, T.; Thomson, N. H.; Chiesa, M. Measuring the True Height of Water Films on Surfaces. *Nanotechnology* **2011**, *22*, 465705.

(56) García, R.; Perez, R. Dynamic Atomic Force Microscopy Methods. *Surf. Sci. Rep.* **2002**, *47*, 197−301.

(57) Hamaker, H. C. The London − Van Der Waals Attraction between Spherical Particles. *Physica* **1937**, *4*, 1058−1072.

(58) Visser, J. On Hamaker Constants: A Comparison between Hamaker Constants and Lifshitz-Van Der Waals Constants. *Adv. Colloid Interface Sci.* **1972**, *3*, 331−363.

(59) Chiou, Y.-C.; Olukan, T. A.; Almahri, M. A.; Apostoleris, H.; Chiu, C. H.; Lai, C.-Y.; Lu, J.-Y.; Santos, S.; Almansouri, I.; Chiesa, M. Direct Measurement of the Magnitude of the Van Der Waals

Interaction of Single and Multilayer Graphene. *Langmuir* **2018**, *34*, 12335−12343.

(60) Calò, A.; Robles, O. V.; Santos, S.; Verdaguer, A. Capillary and Van Der Waals Interactions on Caf2 Crystals from Amplitude Modulation Afm Force Reconstruction Profiles under Ambient Conditions. *Beilstein J. Nanotechnol.* **2015**, *6*, 809−819.

(61) Sahagún, E.; García-Mochales, P.; Sacha, G.; Sáenz, J. J. Energy Dissipation Due to Capillary Interactions: Hydrophobicity Maps in Force Microscopy. *Phys. Rev. Lett.* **2007**, *98*, 176106.

(62) Christenson, H. K. Two-Step Crystal Nucleation Via Capillary Condensation. *CrystEngComm* **2013**, *15*, 2030−2039.

(63) Riedo, E.; Lévy, F.; Brune, H. Kinetics of Capillary Condensation in Nanoscopic Sliding Friction. *Phys. Rev. Lett.* **2002**, *88*, 185505.

(64) Santos, S.; Barcons, V.; Verdaguer, A.; Chiesa, M. Subharmonic Excitation in Amplitude Modulation Atomic Force Microscopy in the Presence of Adsorbed Water Layers. *J. Appl. Phys.* **2011**, *110*, 114902.

(65) Chiesa, M.; Gadelrab, K. R.; Verdaguer, A.; Segura, J.; Barcons, V.; Thomson, N. H.; Phillips, M. A.; Stefancich, M.; Santos, S. Energy Dissipation in the Presence of Sub-Harmonic Excitation in Dynamic Atomic Force Microscopy. *EPL (Europhysics Letters)* **2012**, *99*, 56002.

(66) Amadei, C. A.; Tang, T. C.; Chiesa, M.; Santos, S. The Aging of a Surface and the Evolution of Conservative and Dissipative Nanoscale Interactions. *J. Chem. Phys.* **2013**, *139*, 084708.

(67) Tamalampudi, S. R.; Santos, S.; Lai, C.-Y.; Olukan, T. A.; Lu, J.-Y.; Rajput, N.; Chiesa, M. Rapid Discrimination of Chemically Distinctive Surface Terminations in 2d Material Based Hetero-structures by Direct Van Der Waals Identification. *Rev. Sci. Instrum.* **2020**, *91*, 023907.

(68) Lai, C.-Y.; Santos, S.; Chiesa, M. Machine Learning Assisted Quantification of Graphitic Surfaces Exposure to Defined Environments. *Appl. Phys. Lett.* **2019**, *114*, 241601.

(69) Santos, S.; Lai, C.-Y.; Olukan, T.; Chiesa, M. Multifrequency Afm: From Origins to Convergence. *Nanoscale* **2017**, *9*, 5038−5043.

(70) Santos, S.; Lai, C.-Y.; Amadei, C. A.; Gadelrab, K. R.; Tang, T.-C.; Verdaguer, A.; Barcons, V.; Font, J.; Colchero, J.; Chiesa, M. The Mendeleev-Meyer Force Project. *Nanoscale* **2016**, *8*, 17400−17406.

(71) Lai, C.-Y.; Olukan, T.; Santos, S.; Al Ghaferi, A.; Chiesa, M. The Power Laws of Nanoscale Forces under Ambient Conditions. *Chem. Commun.* **2015**, *51*, 17619−17622.

(72) Santos, S.; Guang, L.; Souier, T.; Gadelrab, K. R.; Chiesa, M.; Thomson, N. H. A Method to Provide Rapid in Situ Determination of Tip Radius in Dynamic Atomic Force Microscopy. *Rev. Sci. Instrum.* **2012**, *83*, 043707−043717.

(73) Garcia, R.; San Paulo, A. Attractive and Repulsive Tip-Sample Interaction Regimes in Tapping-Mode Atomic Force Microscopy. *Phys. Rev. B: Condens. Matter Mater. Phys.* **1999**, *60*, 4961.

(74) Garcia, R.; San Paulo, A. Dynamics of a Vibrating Tip near or in Intermittent Contact with a Surface. *Phys. Rev. B: Condens. Matter Mater. Phys.* **2000**, *61*, R13381−R13384.

(75) Barcons, V.; Santos, S.; Bonass, W.; Font, J.; Thomson, N. H. Mono-Stability of Sharp Tips Interacting with Surface Hydration Layers. *arXiv*, 1506.03961 [cond-mat.mes-hall], 2015.

(76) Santos, S.; Barcons, V.; Christenson, H. K.; Billingsley, D. J.; Bonass, W. A.; Font, J.; Thomson, N. H. Stability, Resolution, and Ultra-Low Wear Amplitude Modulation Atomic Force Microscopy of DNA: Small Amplitude Small Set-Point Imaging. *Appl. Phys. Lett.* **2013**, *103*, 063702−063705.

(77) Chiesa, M.; Gadelrab, K.; Stefancich, M.; Armstrong, P.; Li, G.; Souier, T.; Thomson, N. H.; Barcons, V.; Font, J.; Verdaguer, A.; Phillips, M. A.; et al. Investigation of Nanoscale Interactions by Means of Subharmonic Excitation. *J. Phys. Chem. Lett.* **2012**, *3*, 2125−2129.

(78) Verdaguer, A.; Santos, S.; Sauthier, G.; Segura, J. J.; Chiesa, M.; Fraxedas, J. Water-Mediated Height Artifacts in Dynamic Atomic Force Microscopy. *Phys. Chem. Chem. Phys.* **2012**, *14*, 16080−16087.

(79) Amadei, C. A.; Santos, S.; Pehkonen, S. O.; Verdaguer, A.; Chiesa, M. Minimal Invasiveness and Spectroscopy-Like Footprints for the Characterization of Heterogeneous Nanoscale Wetting in Ambient Conditions. *J. Phys. Chem. C* **2013**, *117*, 20819−20825.

(80) Katan, A. J.; Van Es, M. H.; Oosterkamp, T. H. Quantitative Force Versus Distance Measurements in Amplitude Modulation Afm: A Novel Force Inversion Technique. *Nanotechnology* **2009**, *20*, 165703.

(81) Sader, J. E.; Jarvis, S. P. Accurate Formulas for Interaction Force and Energy in Frequency Modulation Force Spectroscopy. *Appl. Phys. Lett.* **2004**, *84*, 1801−1803.

(82) Amadei, C. A.; Lai, C.-Y.; Heskes, D.; Chiesa, M. Time Dependent Wettability of Graphite Upon Ambient Exposure: The Role of Water Adsorption. *J. Chem. Phys.* **2014**, *141*, 084709.

(83) Santos, S. *Dynamic Atomic Force Microscopy and Applications in Biomolecular Imaging;* University of Leeds: Leeds, UK, 2011.

(84) Voet, D.; Judith, G. V. *Biochemistry;* Wiley, 1995.

(85) Alshehhi, M.; Alhassan, S. M.; Chiesa, M. Dependence of Surface Aging on DNA Topography Investigated in Attractive Bimodal Atomic Force Microscopy. *Phys. Chem. Chem. Phys.* **2017**, *19*, 10231−10236.

(86) Lai, C.-Y.; Tang, T.-C.; Amadei, C. A.; Marsden, A. J.; Verdaguer, A.; Wilson, N.; Chiesa, M. A Nanoscopic Approach to Studying Evolution in Graphene Wettability. *Carbon* **2014**, *80*, 784−792.

(87) Al Mahri, M. A.; Alshehhi, M.; Olukan, T.; Vargas, M. R.; Molini, A.; Alhassan, S.; Chiesa, M. Surface Alteration of Calcite: Interpreting Macroscopic Observations by Means of Afm. *Phys. Chem. Chem. Phys.* **2017**, *19*, 25634−25642.

(88) Lai, C.-Y.; Cozzolino, M.; Diamanti, M. V.; Al Hassan, S.; Chiesa, M. Underlying Mechanism of Time Dependent Surface Properties of Calcite (Caco3): A Baseline for Investigations of Reservoirs Wettability. *J. Phys. Chem. C* **2015**, *119*, 29038−29043.

(89) Chiesa, M.; Lai, C.-Y. Surface Aging Investigation by Means of an Afm-Based Methodology and the Evolution of Conservative Nanoscale Interactions. *Phys. Chem. Chem. Phys.* **2018**, *20*, 19664−19671.

(90) Lai, C.-Y.; Santos, S.; Moser, T.; Alfakes, B.; Lu, J.-Y.; Olukan, T.; Rajput, N.; Boström, T.; Chiesa, M. Explaining Doping in Material Research (Hf Substitution in Zno Films) by Directly Quantifying the Van Der Waals Force. *Phys. Chem. Chem. Phys.* **2020**, *22*, 4130−4137.

(91) Wastl, D. S.; Weymouth, A. J.; Giessibl, F. J. Optimizing Atomic Resolution of Force Microscopy in Ambient Conditions. *Phys. Rev. B: Condens. Matter Mater. Phys.* **2013**, *87*, 245415.